

# Impact of Microdrops on Solid Surfaces for DNA-Synthesis

Claus Maier, Stefan aus der Wiesche and Eberhard P. Hofer  
Department of Measurement, Control and Microtechnology  
University of Ulm, D-89069 Ulm Germany

## ABSTRACT

The miniaturization of chemical synthesis procedures and their integration in complex microfluidic systems is highly interesting both commercially and scientifically. Here, dosing of microdrops for activation or passivation with high accuracy on a substrate or onto each other is investigated as one approach to gain micron size synthesis spots. To optimize such a system it is necessary to investigate the droplet impact with high temporal and spatial resolution.

In this paper we reveal for the first time the impact of microdroplets on solid surfaces in real time. This is done by the visualization of the dynamics with high speed cinematography. Additionally the so gained experimental data is compared to analytical and numerical calculations of this free surface flow.

**Keywords:** Diagnostics of microdevices, microfluidic systems, free surface flow, DNA synthesis

## 1 INTRODUCTION

Microsystems for the chemical analysis and synthesis with a spatial resolution of several microns are of increasing importance. Such microscale devices enable for example tasks such as the identification of unknown DNA fragments or peptides by binding it to samples on a substrate. Several different methods have been introduced to assemble such libraries of addressable and defined sample chemical compounds [1]-[7]. A major concern for all methods are reliability issues, since they should be applied in the field of drug discovery and diagnostics. In order to avoid a decrease of quality due to packaging, shipping and storage, it would be useful to have an apparatus assembling such biochips at the customer's place just before their use.

One possible pathway is the application of microdosing principles from print-on-demand devices [8]. Microdrop-sized loci are formed by dispensing droplets with a diameter of several microns on a substrate. Since surface tension is the dominating effect on such a small length scale no splashes after the drop's impact on the surface of the substrate or on other drops already deposited in this location occur. Therefore it is possible to keep all the reactants assembled on one microspot where they can alter the substrate surface and activate or deactivate the

macromolecular fragments' endings for the next parallel synthesis step applied over the substrate as a whole.

In lot of devices it is necessary to have additional functionality incorporated in the substrate under each microreaction spot, such as heating elements or miniaturized sensors. One approach to fulfill this need for spatial resolution uses e.g. downscaled microtiter plates [9]. In contrast, our way to get such a spatial localization is to combine highly accurate positioning of the macroscopic dosing devices with a chemically altered substrate surface. Controlling the wetting characteristics of the reaction spots repositions microdrops arriving slightly of center.

This paper focuses on the impact of microdrops both on unstructured and structured surfaces and on already deposited droplets. The investigation of such microdrop splashes is important beyond the device development in order to understand the hydrodynamics of microfluidic systems with free surface flows. A prediction via a computational approach is demanding due to the numerical and physical instabilities of microflows dominated by surface tension. This makes it mandatory to compare numerical results to the experiment, which is done here. In the following the visualizations of splashes of microdrops in real-time are compared to numerical and analytical investigations.

## 2 EXPERIMENT

The first report about a visual study of drop impact was published by Worthington [10] in the 19th century. Though for systematic experimental investigations we had to wait for the advent of high-speed camera systems. Engel [11] was one of the first authors publishing high-speed camera recordings of water drops colliding with various solid surfaces. But until today only visualizations of splashing drops down to the mm regime have been presented [12], [13]. Moreover optical magnification in order to access the  $\mu\text{m}$  scale increases the challenge for the speed of the recording systems used. Therefore, the tests presented in this paper have been performed with real high speed cinematography using a microscopic ultra high speed motion analyzer developed by us [14]. As main part of this test rig the commercial ultra high speed camera *Imacon 468* from *DRS Hadland Ltd.* has been optically coupled with a standard microscope *Zeiss Axioplan* via a fiber optic plate. Inside the camera, relay optics channel the light onto a special beam splitter consisting eight-sided mirror pyramid from where it passes to at eight intensified CCD units. The CCD sensors which are arranged in a circle around the

beamsplitter are amplified by micro channel plate (MCP) units mounted in front of the CCD camera sensor. They act as high speed shutters to determine the ultra short exposure time of 10ns of the camera. A self designed light source provides a pulse of 50Mcd generated in a Xenon flash lamp.

Figure 1 shows oil-based ink droplets impacting onto each other. The sequence is a real-time recording with an interframe time of 3μs and an exposure time of 500ns. No impacting drop, including the leading one with a Weber number of 38, causes back bouncing or finger instabilities which would be the case for mm size droplets. They just deform the liquid already attached to the microspot into a flat and regular shape and get soaked into it with no visible oscillations on the observed time scale.

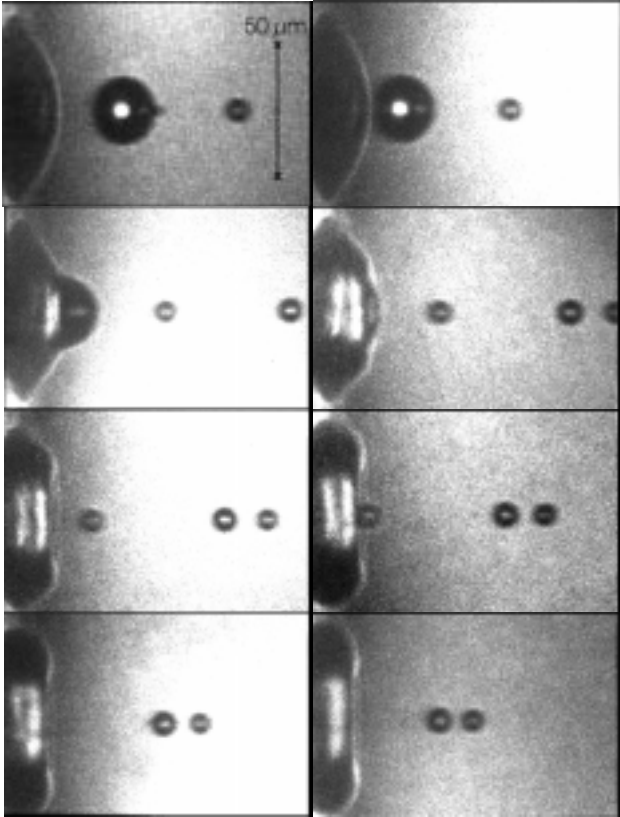


Figure 1: Microdrop impact with 3μs interframe time

### 3 ANALYTICAL TREATMENT

In the following an analytical treatment of surface waves on microdrops and their oscillation behavior is presented. This should give an understanding about possible sources for visible motions of microdrops.

Microdrops are dominated by the surface tension due to the small length scale. This stands in contrast to the common macroscopic treatment. An analytical treatment of such free-surface flows with capillarity effects is possible in the framework of potential theory. Here, the velocity  $\mathbf{w}$  can be obtained as the gradient of the velocity potential  $\Phi$ , i.e.  $\mathbf{w} = \nabla \Phi$  and the continuity equation leads to Laplace's

equation  $\nabla^2 \Phi = 0$  which must be satisfied in the region filled with the fluid. At a rigid boundary, the condition

$$\frac{f\Phi}{fn} = 0 \quad (1)$$

holds, whereas at the free surface the dynamical condition is valid.

$$\frac{f\Phi}{ft} = \frac{T}{\rho} \frac{-f^2 \eta}{fx^2} \Big|_{y=0} \quad (2)$$

In Eq. (4)  $\eta$  stands for the surface elevation at time  $t$  where as  $y = 0$  denotes the unperturbed surface.  $T$  is the surface tension leading to an additional capillarity pressure contribution, and  $\rho$  is the density of the fluid. Additionally, the gravity term is neglected in Eq. (4). Furthermore, the kinematic boundary condition must be satisfied.

$$\frac{f\eta}{ft} = \frac{-f\Phi}{fy} \Big|_{y=0} \quad (3)$$

Assuming periodic time functions  $\exp(-i\omega t)$  the following dispersion relation

$$\omega^2 = \frac{T}{\rho} k^3 \quad (4)$$

for capillarity waves can be deduced from the equations above, if a Fourier component with wave vector  $\mathbf{k}$  is considered for the elevation [15].

#### 3.1 The infinite surface after a Dirac-impulse

At first, the case of an infinite surface after a Dirac-impulse is considered. Since it can be used as an idealization for the dynamics of an impact of a small microdrop with a high velocity onto a very large drop.

In case of a planar symmetry the analytical treatment [15] leads to the following Fourier-integral

$$\eta(x,t) = -\frac{1}{\pi\rho} \int_0^\infty \frac{\sin \omega t}{\omega} \cos kx \, k \, dk \quad (5)$$

which can be further evaluated in the limit case

$$\sqrt{\frac{T}{\rho}} \frac{t}{x^{3/2}} \ll 1 \quad (6)$$

with Kelvin's method of stationary phases to the simple expression

$$\eta = \sqrt{\frac{1}{\pi\rho T x}} \sin \left[ \frac{4}{27} \frac{x^3 \rho}{T t^2} - \frac{\pi}{4} \right] \quad (7)$$

Using the Fourier-Bessel-theorem [16] the more realistic case of cylindrical symmetry leads to the result

$$\eta(r,t) = ar_0 \int_0^\infty J_0(kr) J_1(kr_0) e^{-i\omega(k)t} dk \quad (8)$$

This expression could be further evaluated with Kelvin's method resulting in a similar expression as Eq. (7).

A characteristic elevation profile is plotted in figure 2. It is obvious that capillarity waves differ in several ways from gravity waves. For example, the wave lengths in the far

field decreases. This is why in the micro world droplets behave differently compared to macroscopic regime in which gravity waves dominate. On the other hand the typical length scale of microdrops limits the range of validness of expressions as Eq. (7). This illustrates the restrictions of the analytical approach in case of capillarity phenomena and leads to the necessity to apply numerical treatments.

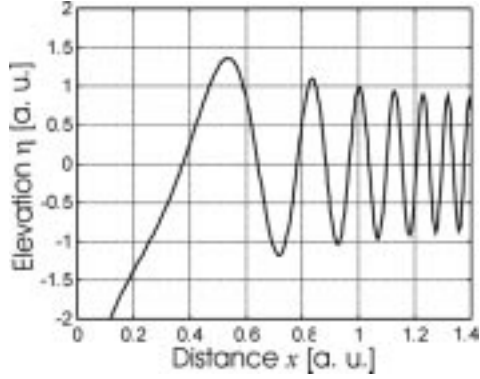


Figure 2: Capillary waves

On the microscale the above considerations show that the typical wavelengths and elevations are extremely small and the strong influence of the surface tension does not permit a visible profile.

### 3.2 Vibrations of drops

The next instructive analytical result is the vibration of a microdrop. This case can be understood as an idealization for the resulting vibrational motion of a drop after collision with a smaller one.

In the literature [15, 17] the linearized analytical treatment leads to the Kelvin modes. Neglecting viscosity and the surrounding air, the eigenmodes are given by

$$\omega^2 = n(n-1)(n+2) \frac{T}{\rho r_0^3} \quad (9)$$

with the unperturbed drop radius  $r_0$  and  $n = 2, 3, \dots$ . However, if the drop is kept at a rigid surface with strong adhesion forces, only higher modes ( $n > 2$ ) can be realized.

## 4 COMPARISON OF NUMERICAL SIMULATION AND EXPERIMENT

Numerical simulations obtained with the commercial CFD code Flow-3D from Flow Science Inc. are compared in figure 3 with the visualized data. This code is specialized for the handling of free fluid surfaces. Taking into account only surface and adhesion forces together with viscous effects, we model the system as one incompressible liquid.

The slices from the 3D-calculations for the outer shape of the liquid surface of the microdrop is in good agreement with the experiment, as can be seen from figure 3.



Figure 3: Simulation and experiment

This gives us the confidence to explore numerically the corresponding flow velocities within an impacting microdrop. Figure 4 shows two sample snapshots from the

velocity fields at the times  $5\mu\text{s}$  and  $17\mu\text{s}$  after the first contact between surface and microdrop. From a more detailed investigation a droplet oscillation period of  $26\mu\text{s}$  can be obtained. This corresponds with the 7<sup>th</sup> eigenmode described in Eq. (9).

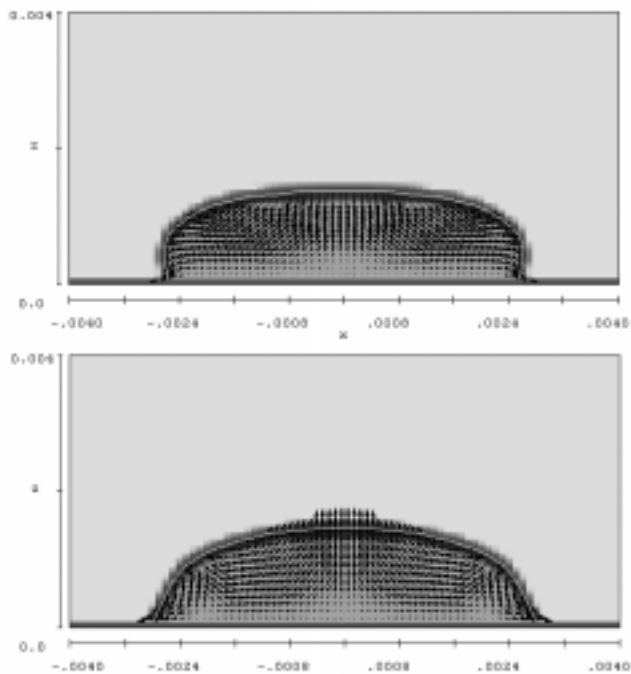


Figure 4: Velocity field at times  $5\mu\text{s}$  and  $17\mu\text{s}$  after impact [ $\mu\text{m}$ ]

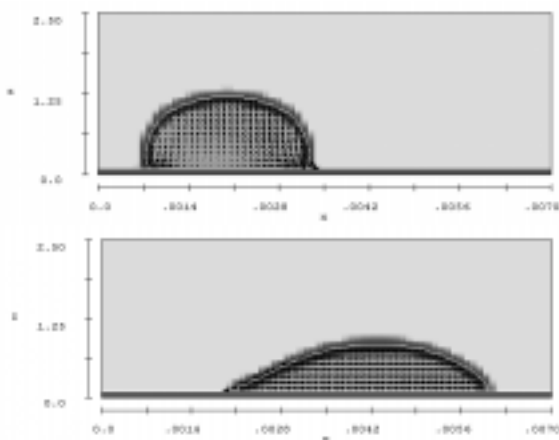


Figure 5: Toluene microdrop impacting on a substrate with locally different wetting properties at  $5\mu\text{s}$  and  $60\mu\text{s}$  after the impact [ $\mu\text{m}$ ]

The simulation can be extended to microdrops impacting on surfaces with spatially changing wetting characteristics. Figure 5 shows slices from a 3D-simulation of a toluene microdrop, in which chemically active compounds might be dissolved. The surface is chosen such that only a microspot with of  $30\mu\text{m}$  in diameter presents a small contact angle of  $5^\circ$  while the rest of the substrate gives a lower surface tension and a contact angle of  $60^\circ$ . The toluene drop hits this spot  $15\mu\text{m}$  off-centered. The calculation shows that during the first  $5\mu\text{s}$  of the impacted

the drop is not influenced by the locally changing surface conditions. In comparison its subsequent movement until the equilibrium is reached takes in our calculation approx.  $100\mu\text{s}$ .

## REFERENCES

- [1] U. Maskos and E.M. Southern, "Oligonucleotide hybridisations on glass supports: a novel linker for oligonucleotide synthesis and hybridisation properties of oligonucleotides synthesised in situ", *Nucleic Acids Res.*, 20, 1679-1684, 1992
- [2] J.W. Jacobs and S.P.A. Fodor, "Combinatorial chemistry-applications of light-directed chemical synthesis", *Tibtech*, 12, 19-26, 1994
- [4] A.C. Pease, D. Solas, E.J. Sullivan, M.T. Cronin, C.P. Holmes and S.P.A. Fodor, "Lightgenerated oligonucleotide arrays for rapid sequence analysis", *Proc. Natl. Acad. Sci. USA*, 91, 5022-5026, (1994)
- [5] G. Wallraff, J. Labadie, P. Brock, R. DiPietro, T. Nguyen, W.Hinsberg and G. McCall, "DNA sequencing on a chip", *Chemtech*, February, 22-32, (1997)
- [6] R.S. Matson J.B. Rampal and P.J. Coassin, "Biopolymer Synthesis on Polypropylene Supports", *Analytical Biochemistry*, 217, 306-331, 1994
- [7] J. Weiler and J.D. Hoheisel, "Combining the Preparation of Oligonucleotide Arrays and Synthesis of High Quality Primers", *Analytical Biochemistry*, 243, 218-227, 1996
- [8] J.D. Baldeschwieler, R.C. Gamble, T.P. Theriault, US Patent, 5,847,105
- [9] J.M. Köhler, R. Pechmann, A. Schaper, A. Schober, T.M. Jovin, M. Thürk, A. Schwienhorst, "Micromechanical Elements for Detection of Molecules and Molecular Design", *Microsystem Technologies* 1, 202-208, 1995
- [10] Worthington, A.M. *Proc. Roy. Soc. London*, 25, 261, 1876
- [11] O.G. Engel, *J. Res. Natl. Bur. Stand*, 54, 281, 1955
- [12] B. Prunet-Foch, F. Legay, M. Vignes-Adler and C. Delmotte, "Impacting Emulsion Drop on a Steel Plate: Influence of the Solid Substrate", *J. of Colloid and Interface Sci.*, 199, 151-168, 1998
- [13] G. Chaidron, A. Soucemarianadin and P. Attane, "Study of the Impact of Drops onto Solid Surfaces", *IS&Ts NIP* 15, 70-73, 1999
- [14] C. Rembe, J. Patzer, E.P. Hofer and P. Krehl, "Realcinematographic visualization of droplet ejection in thermal ink jets", *JIST* 40, 401, 1996
- [15] Sir Horace Lamb, "Hydrodynamics," 6<sup>th</sup> edition, Cambridge, 455-475, 1997.
- [16] A. Sommerfeld, "Mechanik der deformierbaren Medien," 6<sup>th</sup> edition, Harri Deutsch, Frankfurt/M, 172-176, 1992
- [17] S. Chandrasekhar, "Hydrodynamic and Hydro-magnetic Stability," Dover Publications, New York, 466-477, 1981